Title
Microstructural integrity of brain white matter in different substance using populations: Diffusion Tensor Imaging analysis of 4 Tesla MRI data

Permalink
https://escholarship.org/uc/item/59r8j62k

Author
Zou, Yukai

Publication Date
2015

Peer reviewed|Thesis/dissertation

Microstructural integrity of brain white matter in different substance
using populations: Diffusion Tensor Imaging analysis of 4 Tesla
MRI data

by

Yukai Zou

THESIS

Submitted in partial satisfaction of the requirements for the degree of

MASTER OF SCIENCE

in

Biomedical Imaging

in the

GRADUATE DIVISION

of the

UNIVERSITY OF CALIFORNIA, SAN FRANCISCO

Acknowledgement

Abstract

Many individuals with alcohol use disorders (AUD) are chronic cigarette smokers, and the specific contributions of both chronic drinking and smoking to brain injury need to be better understood. A previous analysis of 1.5T diffusion tensor imaging data by Tract-Based Spatial Statistics (TBSS) found significant microstructural injury of brain white matter in 11 smoking alcoholics at 1 week of abstinence. The objectives of this study are to reproduce the 1.5T study with corresponding 4T MRI data from a larger sample of alcoholics (ALC) in recovery and to test the effects of cigarette smoking on microstructural integrity of brain white matter. Corpus callosum, cingulum bundle, fornix, and medial forebrain bundle were chosen as *a priori* regions of interest (ROIs). After TBSS analyses, family-wise error (FWE)-corrected t-statistics showed significant fractional anisotropy (FA) deficits in smoking ALC (sALC) at 1 week of abstinence compared with nonsmoking healthy controls within corpus callosum (body, genu, and splenium), fornix, and medial forebrain bundle, largely replicating the findings at 1.5T. Exploratory uncorrected t-statistics found significant FA deficits in sALC at 1 month of abstinence compared with smoking controls within cingulum bundle, body of corpus callosum, fornix, and medial forebrain bundle; no regional FA difference remained significant after FWE correction. Exploratory uncorrected t-statistics found significant FA decreases and increases in smoking versus non-smoking alcoholics, as well as regional FA decreases in smoking versus non-smoking healthy controls; none of these smoking effects, however, remained significant after FWE correction. The analyses suggest that white matter microstructural integrity in alcoholics is compromised at 1 week of abstinence and may have recovered after 1 month of abstinence, and chronic cigarette smoking may reduce microstructural integrity in both alcoholics and healthy controls.

Table of Contents

List of Tables

List of Figures

1. Introduction

1.1. Alcoholism and Chronic Cigarette Smoking

Alcoholism threatens millions of people's lives around the world. In 2012, there were 17 million adults over 18 years' old in the United States suffering from alcohol use disorder (AUD) (Research Society on Alcoholism, 2015). AUD, according to the definition of Diagnostic and Statistical Manual, is the use of alcohol accompanied by negative consequences across life domains including physical and/or mental health and/or compromise in interpersonal relationships (American Psychiatric Association, 2013). The misuse of alcohol devastates families and burdens the healthcare system, costing approximately $223.5 billion each year in the United States (Research Society on Alcoholism, 2015). In China, alcohol dependence is the third most prevalent mental illness (Cochrane, 2003). Neuroimaging techniques and neurological studies have shown that misuse of alcohol can impair brain areas involved in emotion, memory, and motor coordination, can compromise brain microstructure and normal activity, cause localized and widespread neuronal injury, and damage the intrinsic neuroplasticity/recovery mechanism of injured brain (Meyerhoff, 2014; Research Society on Alcoholism, 2015).

Chronic cigarette smoking is known as the most common comorbidity in AUD. In the United States, around 50 to 90 percent of alcoholics smoke cigarettes (Durazzo et al., 2007), and approximately 400,000 annual deaths are associated with cigarette smoking (Giovino, 2002). Chronic cigarette smoking can mediate the health effects of alcohol dependence. Many studies have shown that chronic cigarette smokers have increased risk of impaired neurobiology and cognition (Bolego et al., 2002; Hawkins et al., 2002; Garey et al., 2004). Together with AUD, chronic cigarette smoking attributes to significant and specific brain injury and health consequences that need to be better studied to be able to treat this common condition more

1

effectively. Studies have found neural recovery in alcoholics with abstinence (Martin et al., 1995; Durazzo et al., 2006; Gazdzinski et al., 2010; Durazzo et al., 2015). However, little knowledge exists about how smoking affects the recovery of microstructural integrity of brain white matter. The specific contributions of both chronic drinking and smoking to brain injury need to be better understood.

1.2. Diffusion and Diffusion Tensor Imaging (DTI)

Diffusion is the thermal (Brownian) motion of molecules. In human brain, water molecules occupy most of the tissue, and water protons provide most of the signals in MR images (Chanraud et al., 2010). Diffusion Tensor Imaging (DTI) is a non-invasive MR imaging technique that provides a comprehensive approach to probe microstructure in the order of about 10µm (Mori and Zhang, 2006), assessing the microstructural integrity of white matter quantitatively through measuring the magnitude, anisotropy, and directionality of water diffusion via a tensor model of diffusion (Hess and Mukherjee, 2007; Mukherjee et al., 2008). The diffusion tensor is computed to characterize the directionality of water diffusion. The tensor is composed of three eigenvectors, and each eigenvector characterizes the diffusion in one of the three cardinal tensor directions (Chanraud et al., 2010). The lengths of the three axes are defined as eigenvalues (λ_1, λ_2, and λ_3). Mean diffusivity (MD) and fractional anisotropy (FA) can be calculated from the three eigenvalues for each voxel of the diffusion image:

$$MD = \frac{\lambda_1 + \lambda_2 + \lambda_3}{3}, FA = \sqrt{\frac{(\lambda_1 - MD)^2 + (\lambda_2 - MD)^2 + (\lambda_3 - MD)^2}{2(\lambda_1^2 + \lambda_2^2 + \lambda_3^2)}}.$$ FA is a scalar value ranging from 0 (isotropic) to 1 (anisotropic), which reflects fiber density and myelination (Beaulieu, 2002); MD, also known as apparent diffusion coefficient (ADC), reflects cellular density and extracellular volume (Beaulieu, 2002). Voxels with low FA values indicate less directionality of water diffusion, i.e. small anisotropy, which may be due to demyelination (Pfefferbaum and Sullivan,

2005). Revealing rich information for the complex neural network, DTI has greatly enhanced our understanding of the mechanisms or type of injury underlying many neurodegenerative, neurocognitive, and psychiatric disorders (Mori and Zhang, 2006; Kuceyeski et al., 2013).

1.3. Tract-Based Spatial Statistics (TBSS)

One of the standard approaches for analyzing DTI data is Tract-Based Spatial Statistics (TBSS) (Smith et al., 2006; Bach et al., 2014). TBSS is a voxel-based image analysis technique combining the strengths of both voxel-wise and tractography-based analyses. In TBSS, nonlinear image transformation is applied to FA maps to avoid distortion effects due to affine image registration; after that, a mean FA skeleton is created through averaging and localizing the 3×3×3 neighboring voxels into a single voxel that becomes part of that skeleton. As such, the mean FA skeleton represents the major fiber bundles connecting different cortical brain regions. By reducing the dimension and project volumetric FA data onto the skeleton instead of comparing voxel by voxel across images, partial volume effects can be reduced with increased statistical power (Smith et al., 2006), and regional microstructural white matter integrity can be compared at the group level (Bach et al., 2014).

TBSS analysis has been widely practiced to delineate differences in local white matter microstructure (Benedetti et al., 2015; Brewster et al., 2015). Taking alcohol dependence as an example, in 2009, Yeh et al. first reported microstructural abnormalities of brain white matter in alcohol-dependent populations using TBSS, including in cortical-striatal fibers, frontal white matter, and limbic pathways (Yeh et al., 2009). Yeh's study acquired and analyzed 1.5 Tesla MRI data from a relatively small sample size. Since then, alcohol dependence has been further investigated using TBSS to explore microstructural integrity in alcoholics (Kuceyeski et al.,

2013), Korsakoff's syndrome (Segobin et al., 2015), in comorbid post-traumatic stress disorder (Durkee et al., 2013), and in binge alcohol consumption (Pfefferbaum et al., 2015).

1.4. Objectives

The objectives of this thesis were to replicate Yeh's 1.5T DTI study with a new set of DTI data obtained at 4T and to conduct further TBSS analyses with 4T DTI data obtained from alcohol dependent individuals in recovery, to test for effects of cigarette smoking on white matter microstructural integrity of alcoholics and healthy controls, and to test for evidence of recovery of white matter microstructural integrity during abstinence from alcohol.

A schematic diagram of the study design is shown in **Figure 1**. To perform the study, raw data were gathered (staged) and preprocessed to yield images of DTI metrics. This phase was followed by formulating specific aims and hypotheses as outlined in the objectives above and by grouping raw data from individual cases (subjects or time points during abstinence) into different datasets. After that, TBSS analyses were conducted on each dataset to investigate FA differences on the group's skeleton. Future analyses will follow the same scheme with datasets prioritized based on the interest of the scientific question and the number of available data sets to address the question. The current thesis was composed from the analyses of several such datasets.

1.5. Specific Aims

Based on the objectives and available datasets, this thesis focused on three specific aims: First, we aimed at validating Yeh's 1.5T findings with new 4T DTI data, by comparing voxels with FA values in 11 smoking alcoholics (ALC) at 1 week of abstinence to voxels with the values in 11 non-smoking controls. Second, we aimed at investigating the microstructural white matter integrity of 1-month abstinent alcoholics, using a larger 4T DTI dataset and comparing voxels with FA values in 27 smoking ALC at 1 month of abstinence to the values in 37 smoking

controls. Third, we aimed at investigating the effects of smoking on microstructural white matter integrity in alcoholics and healthy controls, by comparing voxels with FA values in 21 non-smoking ALC to the values in 27 smoking ALC (both groups at 1 month of abstinence), and by comparing voxels of FA values between 27 non-smoking and 37 smoking controls. The demographic information of each group is summarized in **Table 1**.
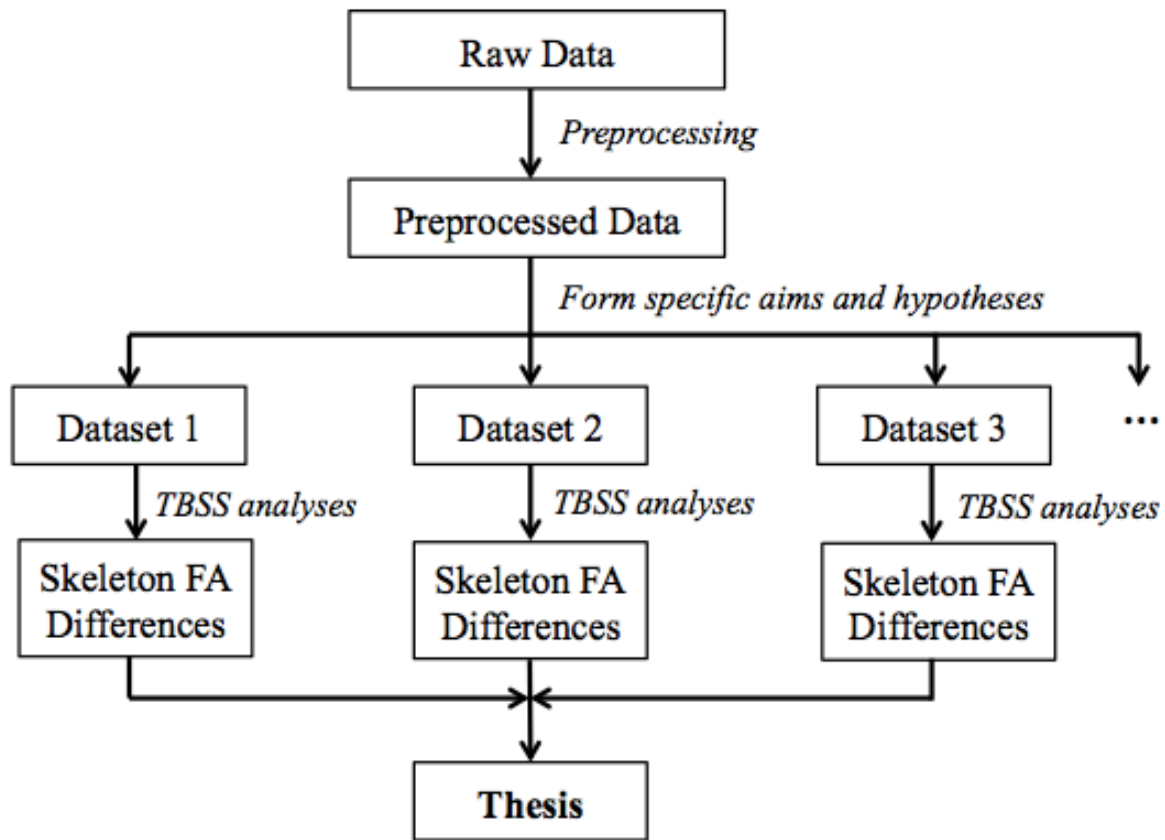
Figure 1. Schematic Diagram of Study Design. Raw data were first gathered (staged) and preprocessed to yield images of DTI metrics, followed by formulating the specific aims and hypotheses. Raw data were grouped from individual cases (subjects or time points during abstinence) into different datasets. After that, TBSS analyses were conducted on each dataset to investigate FA differences on the group's skeleton. The current thesis was composed from the analyses of several such datasets.

	sCON	nsCON	sALC	sALC	nsALC
Duration of Abstinence	--	--	1 week	1 month	1 month
Mean Age (SD)	47.0 (10.1)	48.1 (12.1)	51.8 (6.6)	49.3 (8.8)	52.6 (13.8)
Number of Subjects (Females)	37 (5)	28 (3)	11 (2)	27 (2)	21 (5)
Mean No. Drinks per Month last Year (SD)	21 (20)	17 (17)	402 (144)	394 (249)	279 (166)
Mean No. Drinks per Month over Life Time (SD)	25 (14)	19 (14)	261 (124)	229 (108)*	147 (89)
Mean Fagerstrom Score (SD)	4.7 (1.6)	--	4.6 (1.9)	4.3 (1.8)	--
Mean No. Cigarettes per Day (SD)	18 (6)	--	17 (8)	16 (8)	--
Mean Years of Smoking at Current Level (SD)	13.8 (11.0)	--	14.7 (11.9)	19.1 (13.9)	--

Table 1. Demographics of study populations. Information on smoking controls (sCON), non-smoking controls (nsCON), smoking alcoholics (sALC), and non-smoking alcoholics (nsALC) are summarized. SD = standard deviation. * $p < 0.05$ compared to nsALC.

2. Methods

2.1. Subjects

The current 4 Tesla MRI datasets at the Center for Imaging of Neurodegenerative Diseases (CIND) contain around 350 DTI and structural (both T1 and T2) data sets from different projects, consisting of both cross-sectional and longitudinal data. There were treatment seeking alcoholics (ALC) at 1 week (n = 30), 4 weeks (n = 90), and 6-9 months of abstinence (n = 40) including smokers and non-smokers, with available relapse status at 6 – 9 months for all 90 ALC at 4 weeks of abstinence. There were polysubstance users (treatment-seeking alcoholics who were also abusing illicit drugs such as cocaine and methamphetamine) at 1 month of abstinence (n = 31), with available relapse status at 4 months of abstinence. There were smoking heroin addicts on buprenorphine maintenance therapy (n = 22), and healthy controls (n = 80), including smokers and non-smokers.

2.2. Data Acquisition

MRI data were acquired on a 4 Tesla Bruker MedSpec system with a Siemens Trio console (Siemens, Erlangen, Germany) using an 8-channel transmit-receive head coil. The diffusion-weighted data were acquired with a dual spin echo echo planar imaging (EPI) sequence that used 6 diffusion-encoding directions at b = 800 s/mm^2 and one at b = 0 s/mm^2, acquired from 40 3.0mm thick interleaved slices (no slice gap) and 128×112 matrix size (final voxel size 2.0×2.0×3.0 mm^3). Twofold parallel imaging acceleration was used to reduce geometrical distortions and four scans were averaged to boost signal to noise. Detailed descriptions can be found in Kuceyeski's work (Kuceyeski et al., 2013).

2.3. DTI Processing

The diffusion tensor of each voxel in the FA map was computed using a python-based preprocessing pipeline (TEEM) (http://teem.sourceforge.net/) developed at the CIND (CIND, 2012). Prior to TEEM pipeline, the T1 and T2 datasets were processed and archived through expectation maximization segmentation (EMS) pipeline. During EMS processing, the T1 images underwent bias correction and skull stripping, whereas the oblique axial T2 images were resampled and resliced. The processed T1 image will be the template for up-scaling the DTI data, whereas the processed T2 image will be registered to the b=0 image for correcting the geometric distortion induced by EPI sequence. During TEEM preprocessing, the DTI, T1, and T2 data of the same case were staged into the pipeline. The data staged for each case had to be acquired at the same scanning session; when multiple DTI, T1, and T2 datasets were present at the same time point, the dataset with least motion artifacts in the T1 data was chosen. Then, a b=0 image mask was generated semi-automatically, which requires manual edits so that the mask covers only the brain tissue but excludes non-brain areas such as meninges. After creating the b=0 image mask, image distortions due to eddy currents and head motion were corrected, followed by affine image registration and geometric distortion correction. Finally, slice-wise maps of eigenvectors, FA and MD were computed.

Quality control was conducted at the end of preprocessing to visually check whether the case can proceed to TBSS analysis. If the T2 mask did not cover the whole brain volume, the case was marked as "failed", and the EMS pipeline was relaunched to try to solve the problem (CIND, 2010). Next, the registration of T2 mask to b=0 image was checked; poor registration causes DTI information loss in subsequent processing, therefore any such cases were marked as "failed", and the TEEM pipeline was relaunched to help solve the problem. By comparing the overlays of the

distortion corrected b=0 image and T2 mask, the correction of geometric distortion was examined to ensure that all the tensor information can be reconstructed from DTI data. Cases with a severe mismatch of the overlays were marked as "failed" and cases that passed quality control with "partial failure" in specific regions are explained below in Discussion. Finally, the final FA map was checked to see whether acquisition field-of-view cutoffs occur in white matter regions or whether FA values were presented in non-brain regions (CIND, 2012); in either situation, the case was marked as "failed", and relaunching the EMS pipeline for the failed cases and/or re-editing of b=0 image mask often solved the initial problem.

2.4. TBSS Analysis

FA maps were submitted to FSL's TBSS (Smith et al., 2006) for voxelwise, group-level analysis. A nonlinear transformation algorithm was applied to align individual images to the FMRIB58_FA template supplied with FSL (http://fsl.fmrib.ox.ac.uk/fsl/fslwiki/FMRIB58_FA). This template contains 58 high-resolution FA volumes from healthy male and female subjects aged 20-50 years. Next, all warped FA images were normalized to the Montreal Neurological Institute standard space (MNI152 T1, 1mm spatial resolution). A mean FA image was created from all data in the datasets and thinned to generate a mean FA skeleton that represents the locally maximal FA values. The mean FA skeleton was thresholded at $FA > 0.20$ to reduce the likelihood of partial volume effects between the borders of different tissues, yielding a subject-specific skeleton with approximately 80,000 voxels. Perpendicular to the mean skeleton, maximal FA values were identified over a $3 \times 3 \times 3$ voxel neighborhood and then projected onto the skeleton according to a distance map, which further reduces partial volume effects (Smith et al., 2006). The resulting mean FA skeletons were fed into voxelwise permutation-based cross-subject statistics.

2.5. Statistical Analysis

Voxelwise analyses were conducted using unpaired *t*-tests controlling for participant age (because FA decreases with age), drinking severity (average monthly drinks in last year, average monthly drinks over life time) for smoking analyses in ALC and CON, and nicotine dependence scores (total Fagerstrom score, total cigarettes per day, years of smoking at current level) for drinking analyses in comparing ALC vs. CON, via R statistics (R Development Core Team, 2011) and the FSL permutation-based program Randomise (Randomise v2.9, http://fsl.fmrib.ox.ac.uk/fsl/fslwiki/Randomise) (Nicholes & Holmes, 2002); covariates were included in the final model only if they were significantly different between the groups examined. 5000 random permutations were used to correct for multiple comparisons. Type I error was controlled via threshold-free cluster enhancement (TFCE) (Smith and Nichols, 2009). The voxel-wise cross subject statistics were corrected using a family-wise error (FWE) approach with the statistical significance threshold set at $p<0.05$ and an empirical null distribution generated by the 5000 permutations for each contrast. Significant neuroanatomical regions on the skeleton were identified manually by comparison to a white-matter label atlas available within the TBSS software (JHU ICBM-DTI-81, http://cmrm.med.jhmi.edu/) (Mori et al., 2005). In reporting results of the analyses, special attention was paid to the voxels within four *a priori* defined regions: the cingulum bundle, corpus callosum, fornix, and medial forebrain bundle, regions that have been shown repeatedly to be affected in DTI studies of substance using populations (Wang et al., 2011; Durkee et al., 2013; Kochunov et al., 2013; Ma et al., 2015; Segobin et al., 2015; Yu et al., 2015). In all analyses, $p<0.05$ was considered statistically significant.

3. Results

3.1. Highfield Replication of Yeh's 1.5T TBSS DTI Analyses

At 4T, we replicated Yeh's 1.5T TBSS study of lower regional FA in smoking ALC at one week of abstinence compared to non-smoking CON (Yeh et al., 2009); the findings were significant after FWE correction (**Figure 2**). Significant FA deficits were found within ROIs corresponding to corpus callosum (body, genu, and splenium), fornix, and medial forebrain bundle (anterior thalamic radiation). Additional significant FA deficits were found within anterior corona radiata, external capsule, inferior fronto-occipital fasciculus, and superior longitudinal fasciculus. These regions were similar to those found affected earlier at 1.5T. In further analyses, no region of significantly higher FA in ALC versus CON was observed.
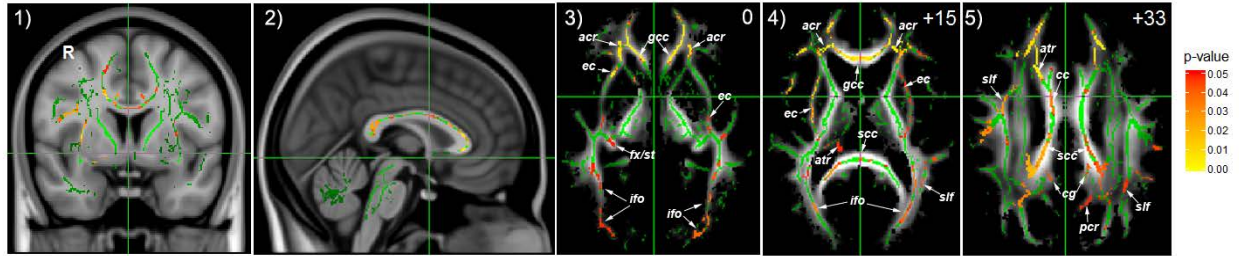
Figure 2. 4T replication of previous TBSS DTI work at 1.5 T (Yeh et al., 2009): Smoking ALC at 1 week of abstinence < non-smoking CON: FWE corrected *t*-statistical maps (red-yellow, p < 0.05, 5000 permutations) of FA group differences. Panel 1) is sagittal and Panel 2) coronal view overlaid on the mean FA skeleton (green) and the MNI template ($1 \times 1 \times 1\ mm^3$), with the anterior commissure centered at the cross bars. Panels 3), 4), and 5) are representative axial views of *t*-statistical maps, with the number at the top-right corner indicating the distance (in mm) from the anterior commissure. *acr* = anterior corona radiata, *atr* = anterior thalamic radiation, *cg* = cinglum, *ec* = external capsule, *fx/st* = fornix/ stria terminalis (cannot be resolved with current resolution), *gcc* = genu of corpus callosum, *ifo* = inferior frontal-occipital fasciculus, *pcr* = posterior corona radiata, *scc* = splenium of corpus callosum, *slf* = superior longitudinal fasciculus.

3.2. 4T Follow-up TBSS DTI Analyses, Uncorrected for Multiple Comparisons

This set of analyses included a larger group of ALC from whom DTI data were obtained after about 1 month (4 weeks) of abstinence from alcohol. Before corrections for multiple comparisons, the whole-brain TBSS analysis revealed regions of significant FA deficits within smoking ALC at 1 month of abstinence compared with smoking CON (**Figure 3A**), within ROIs corresponding to cingulum bundle, medial forebrain bundle (anterior thalamic radiation), and fornix (striatal terminalis) ($p < 0.05$, uncorrected). FA was also reduced within body of corpus callosum, external capsule, forceps minor, and superior longitudinal fasciculus ($p < 0.05$, uncorrected). When comparing this data in 1-month-abstinent alcoholics (**Figure 3A**) to the data described above in 1-week-abstinent alcoholics (**Figure 2**), we no longer find FA reductions within genu and splenium of the corpus callosum), inferior fronto-occipital fasciculus and anterior corona radiata. This and other differences in the t-statistical maps suggest regional recovery from microstructural injury between 1 and 4 weeks of abstinence from alcohol.

We further tested the effects of smoking on regional FA measures among ALC at 1 month of abstinence (**Figures 3B and 3C**). According to **Figure 3B**, smoking ALC compared to nonsmoking ALC had FA deficits corresponding to ROIs of medial forebrain bundle (anterior thalamic radiation) ($p < 0.05$, uncorrected); FA deficits were also found within inferior longitudinal fasciculus and uncinate fasciculus ($p < 0.05$, uncorrected). However, as can be appreciated in **Figure 3C**, smoking ALC compared to non-smoking ALC also had regions of higher FA in left medial forebrain bundle (anterior thalamic radiation), left external capsule, left posterior limb of internal capsule, and left superior corona radiata (all $p < 0.05$, uncorrected).

In additional analyses, we tested for smoking effects among healthy controls (CON) (**Figure 3D**). FA deficits were found in smoking CON compared with non-smoking CON, within ROIs

13

corresponding to corpus callosum (body, genu, and splenium), medial forebrain bundle (anterior thalamic radiation), and superior cingulum bundle (p < 0.05, uncorrected); additional FA deficits were found within external capsule, forceps minor, inferior frontal-occipital fasciculus, inferior longitudinal fasciculus, superior longitudinal fasciculus, superior thalamic radiation, and posterior corona radiata (p < 0.05, uncorrected). In contrast to the comparisons in ALC, there were no regions in which FA was found significantly higher in smoking compared to non-smoking CON.
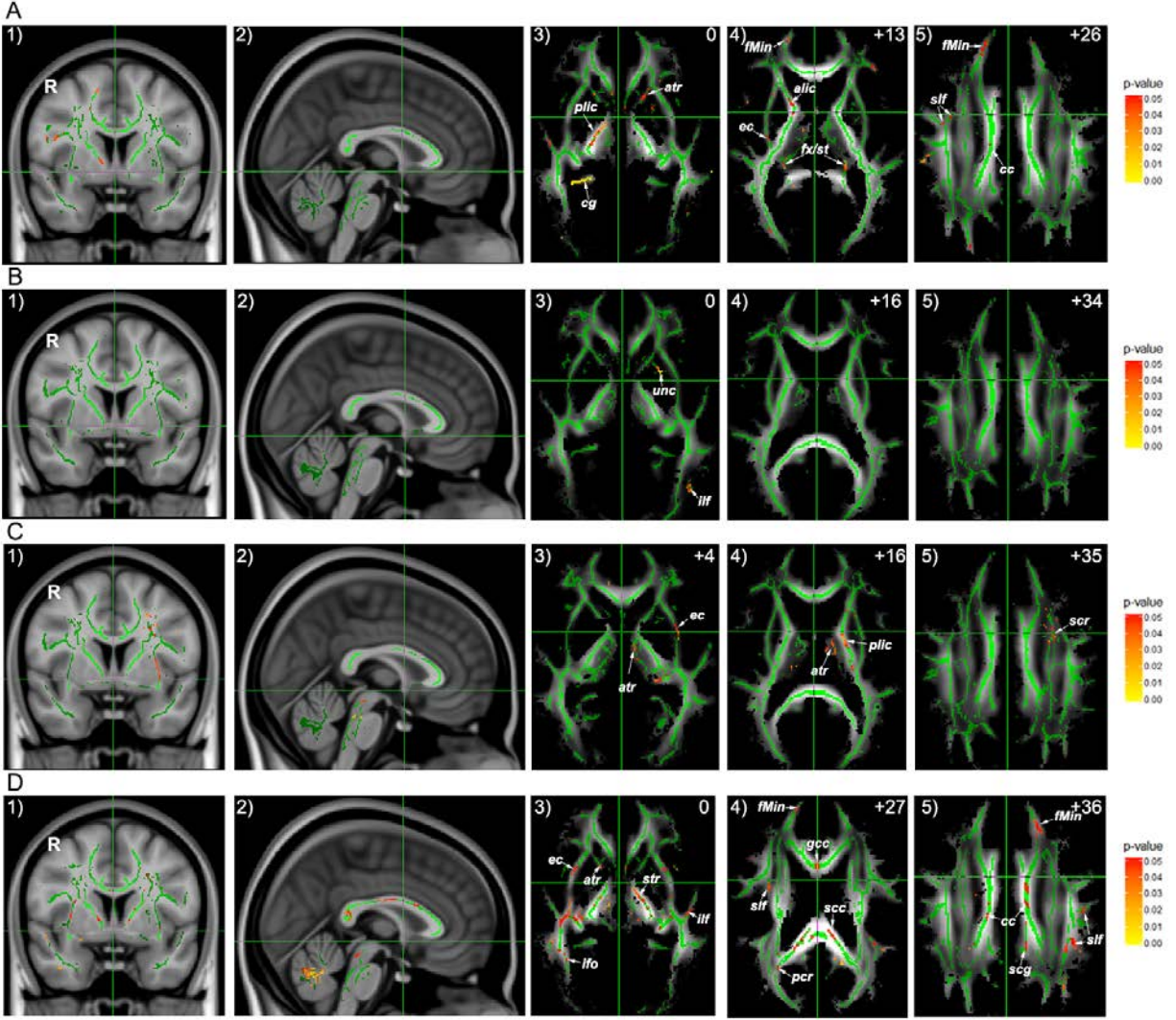
Figure 3. Uncorrected *t*-statistical maps of 4T follow-up TBSS DTI data: (A) Smoking ALC at 1 month of abstinence < smoking CON: (B) smoking ALC at 1 month of abstinence < non-smoking ALC at 1 month of abstinence, (C) non-smoking ALC at 1 month of abstinence < smoking ALC at 1 month of abstinence, and (D) smoking CON < non-smoking CON. All maps are uncorrected *t*-statistical maps (red-yellow, p < 0.05) of FA group differences. Panel 1) sagittal and Panel 2) coronal views overlaid on the mean FA skeleton (green) and the MNI template ($1 \times 1 \times 1\ mm^3$), with the anterior commissure centered at the cross bars. Panels 3), 4), and 5) are representative axial views of the *t*-statistical maps, with the number at the top-right corner indicating the distance (in *mm*) from the anterior commissure. *alic* = anterior limb of internal capsule, *atr* = anterior thalamic radiation, *cc* = corpus callosum, *ec* = external capsule, *fMin* = forceps minor, *fx* = fornix, *gcc* = genu of corpus callosum, *ifo* = inferior fronto-occipital fasciculus, *ilf* = inferior longitudinal fasciculus, *pcr* = posterior region of corona radiata, *plic* = posterior limb of internal capsule, *rlic* = retrolenticular part of internal capsule, *scc* = splenium of corpus callosum, *scg* = superior region of cingulum, *slf* = superior longitudinal fasciculus, *str* = superior thalamic radiation, *unc* = uncinate fasciculus

15

3.3. 4T Follow-up TBSS DTI Analyses after FWE Correction

After FWE correction, there was no region of significantly lower FA in smoking ALC at one month of abstinence versus smoking CON (**Figure 4A**), smoking ALC versus non-smoking ALC at one month of abstinence (**Figure 4B**), and smoking versus non-smoking CON (**Figure 4C**). Similarly, when testing for the inverse contrasts (higher FA) across the three group comparisons, no significant regional FA increases were observed after FWE corrections.
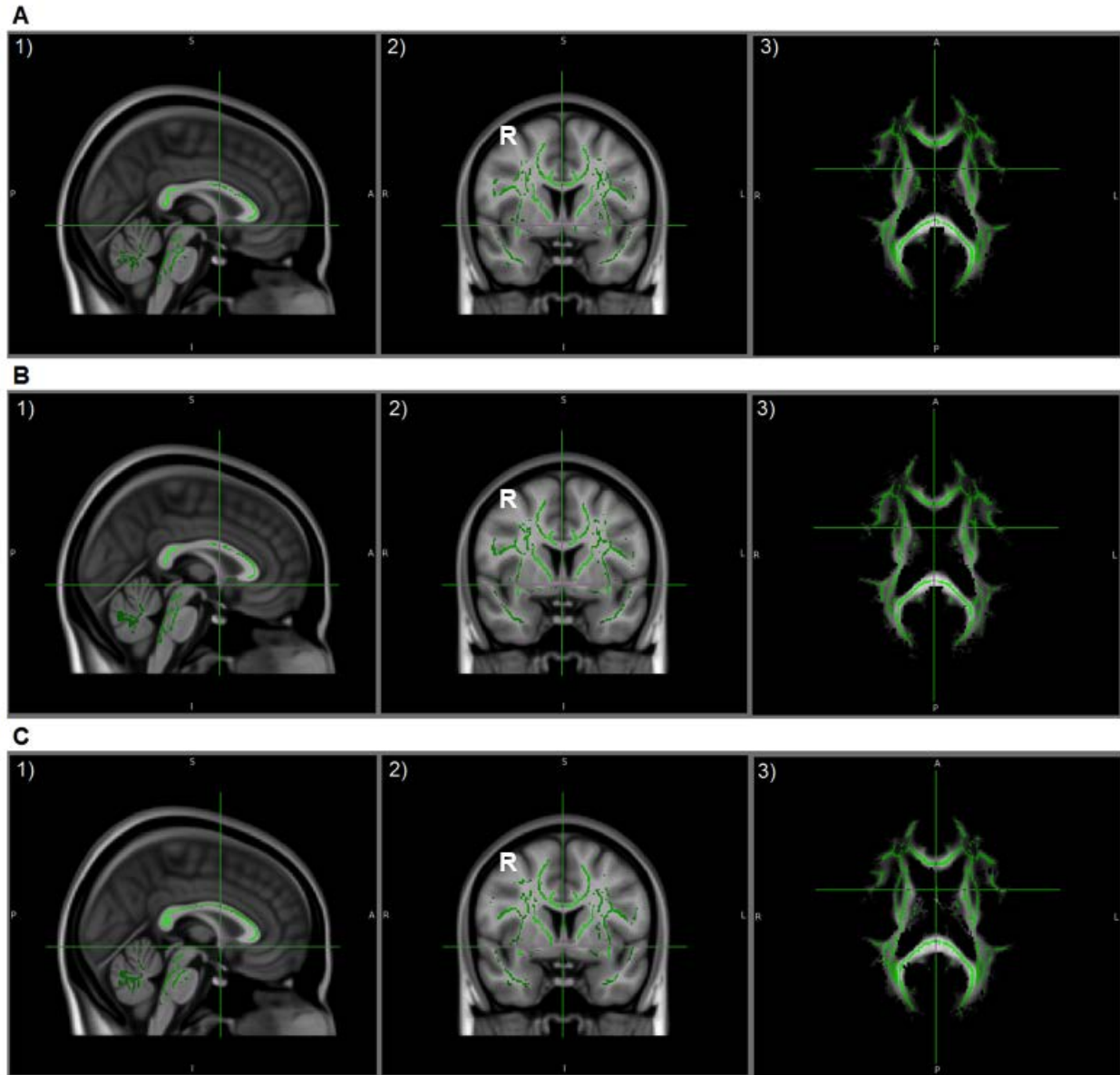
Figure 4. FWE corrected *t*-statistical maps (p < 0.05, 5000 permutations) of the data shown in Figure 3. There are no statistically significant FA group differences for (A) smoking ALC at 1 month of abstinence vs. smoking CON, (B) smoking ALC at 1 month of abstinence vs. non-smoking ALC at 1 month of abstinence, and (C) smoking CON vs. non-smoking CON. Panel 1) sagittal, 2) coronal, and 3) axial representative views overlaid on the mean FA skeleton (green) and the MNI template ($1 \times 1 \times 1\ mm^3$), with the anterior commissure centered at the cross bars.

4. Discussion

4.1. Data Interpretation

Consistent with the peer-reviewed findings in Yeh's 1.5T TBSS analyses (Yeh et al., 2009), there were significant FA deficits in smoking ALC at 1 week of abstinence compared with non-smoking controls (**Figure 2**). Therefore, these replication findings indicate that the methods used for 4T DTI data processing were validated. In general, lower regional FA reflects a compromised white matter microstructural integrity associated with comorbid alcohol and tobacco consumption.

According to **Figures 3B**, **3C**, and **3D**, the findings of widespread albeit uncorrected FA differences indicate that smoking may have different effects on white matter microstructure in ALC (both higher and lower regional FA) and CON (only lower regional FA). Higher FA, in general, represents better coherence and microstructure of fibers. Several recent papers describe both lower and higher regional FA in healthy chronic cigarette smokers compared to non-smokers (Paul et al., 2008; Gazdzinski et al., 2010; Gons et al., 2011; Liao et al., 2011; Hudkins et al., 2012; Lin et al., 2013), including a recent TBSS study in young and healthy smokers that reported increased FA within ROIs similar to our findings but all in the right hemisphere (Yu et al., 2015). However, considering the different study populations, plus the fact that our smoking effects disappear after multiple comparison correction, we cautiously conclude in this thesis that smoking affects brain microstructure in ALC and that the effects may be different from those detected in controls, a finding not yet described in the literature. Smoking effects on brain microstructure in ALC are consistent with previous findings of greater cognitive and neurobiological deficits in smoking ALC versus non-smoking ALC (reviewed in Durazzo et al.,

2010) and with our preliminary 1.5T DTI report of differential recovery from microstructural injury in smoking and non-smoking ALC (Gazdzinski et al., 2010) .

In addition, we found less significant and fewer regions of FA deficits in ALC at 1 month of abstinence (compared to a large group of controls, see **Figure 3A**) than in ALC at 1 week of abstinence (compared to a small group of controls, see **Figure 2**). Specifically, FA differences in *a priori* defined regions of 1-week-abstinent ALC (genu and splenium of corpus callosum) were not any longer found in 1-month-abstinent ALC. It is possible that microstructural injury in those regions resolved with abstinence, which is consistent with previous findings of macrostructural, metabolic, and cognitive recoveries in abstinent ALC (Martin et al., 1995; Bendszus et al., 2001; Parks et al., 2002; Durazzo et al., 2006; Cardenas et al., 2007; Mon et al., 2009; Gazdzinski et al., 2010; Durazzo et al., 2015). However, as separate tests and different comparison groups were used, it is also possible that such differences may simply be due to chance and not significant upon further study. Clearly, our future studies will use the 16 ALC with DTI data from two time points (at 1 week and 4 weeks of abstinence) to assess longitudinal FA changes or more complex mixed effects analyses in larger samples unbalanced across time points.

4.2. Critical Issues in DTI Processing

The accuracy of TBSS analysis relies heavily on the quality of the DTI data, therefore the preprocessing and quality control are very critical; either not strictly following the established processing protocols or not paying sufficient attention to detail can lead to no outcome, non-reproducible results, or systematic errors and false discoveries.

Using the TEEM pipeline for DTI data processing allows consistent data processing with rigorous quality control at various steps. However, TEEM pipeline cannot be launched when the T1 and T2 data are not fully processed and archived through the Expectation Maximization

Segmentation (EMS) pipeline. In EMS, image processing and archiving can be conducted through either manual or automated mode. However, the manual mode will not create a processed T1 file, without which the TEEM pipeline cannot be launched. In addition, some processed T1 files created several years ago cannot be recognized by the current TEEM pipeline. Therefore, both the existing algorithms for EMS and TEEM pipeline required some modifications to enable automated preprocessing.

Several study participants were scanned more than once at the same time point so that multiple DTI, T1, and T2 datasets exist. In such cases, the quality of T1 image was critically evaluated to determine which dataset to be staged into TEEM pipeline. Generally, the T1 image with the least motion artifacts was chosen. Although this criterion proved efficient and robust, the selection assumed a good quality of DTI and T2 data, which did not always hold. Therefore, upon further inspection, some data sets had to be excluded for further analyses.

4.3. Limitations

Although this study used a dataset obtained at higher static magnetic field strength and the sample sizes were significantly larger than previous analyses in alcoholics (Yeh et al., 2009), there are several limitations. First, the current 4T DTI data are encoded in 6 directions only, because the longitudinal studies were initiated about 10 years ago when 6 directions were state-of-the-art on Siemens equipment. While theoretically, tractography analysis could be performed with such data, good and meaningful tractography analyses require a minimum of about 30 directions (Mukherjee et al., 2008). For these reasons, we chose to analyze the DTI data using the TBSS approach. In addition, as study participants were US veterans, only a few females were included in each group (**Table 1**), which prevents us from making comparisons between genders. Furthermore, as for some other studies listed in Future Investigations below (e.g. longitudinal

microstructural recovery), the currently available DTI data may still suffer from limited statistical power as data from two or three time points are not available from a larger number of substance users during abstinence; relapse and attrition typically reduce longitudinal study participation, especially in substance users.

There are also limitations in the current TEEM pipeline. Indeed, TEEM pipeline has effectively saved time on preprocessing large available data sets so that one only needs to focus on quality control of the outcomes; however, eddy currents with shorter decays cannot be recognized by TEEM pipeline at present, which will introduce image blurring effects; distortions may be induced in the first few DTI slices where eddy currents still exist between consecutive slices. As for distortion correction, the current TEEM pipeline uses "variation matching" method (CIND, 2012), which – like most other methods – does not correct for pixel aliasing, which leads to calculation errors of the local diffusion tensor. In addition, the nonlinear deformations can change topological information and distort the original fiber tracts to some unspecified degree (CIND, 2012).

Quality control after preprocessing is subjective and may directly influence the DTI data. Take evaluating the quality of geometric distortion correction as an example: in almost every case, the correction was imperfect in frontal and/or temporal lobes, where the brain tissues were not covered by the corrected T2 mask, which may contribute to loss in DTI data. In this situation, the quality control program offered an option to pass the case with "partial failure" in the specific areas. Although frontal and temporal lobes are cortical regions and do not contain useful FA information in this implementation of the DTI protocol, judgement is subjective and hard to make in regions where geometric distortions are not corrected but white matter may exist. We did not come across such situation in the study, but we did observe several cases where

geometric distortions were not corrected, due to either the T2 mask not covering the whole brain, or the T2 mask did not register to b=0 image; both situations, however, were fixed after re-running the cases through the EMS and TEEM pipelines. To summarize, carefully conducted quality control, although potentially subjective in cases, ensures the generation of reproducible TBSS outcomes that contributes to meaningful results.

Despite the popularity of TBSS, there are several technical challenges that need to be addressed. Because the current DTI images cannot resolve merging fibers (e.g. joint between corpus callosum and corona radiation, medial fiber bundle and anterior thalamic radiation, fornix and striatal terminalis, etc.), TBSS fails to estimate accurate microstructural integrity in those regions (Bach et al., 2014). In addition, TBSS processes FA maps without orientation information; therefore the skeleton FA maps cannot interpret anatomical connectivity between different brain regions. Improvements to the above challenges have been proposed, including the incorporation of direction information in TBSS, or using high angular resolution diffusion imaging (HARDI) to recover multiple fiber orientations (Hess and Mukherjee, 2007). Another technical challenge is that TBSS is mostly restricted in estimating microstructural changes and cannot be used to estimate group FA where morphological changes occur, for instance, the existence of brain tumor. Such gross morphological alterations were not observed in our study participants. Lastly, image registration is a critical but easily underestimated issue; there are many situations where the default template in TBSS, FMRIB58_FA, is not applicable, such as registering pediatric brain images, where other registration techniques are required (for review see Bach et al., 2014). In our case, however, our study participants were of similar age as the contributors to the template we used. Alternatively, we could have created our own template based on the available control data. This, however, would have taken more time and effort than

was available for this thesis. Overall, it is important to be aware of these technical issues, as ignorance or unawareness can lead to systematic errors, complicating interpretation of findings or even leading to false discoveries.

4.4. Future Investigations

In the future, our first analysis, which was primarily aimed at replicating Yeh's smaller study performed at 1.5T, can be extended by using all 4T DTI data sets available from alcoholics at 1 week of abstinence, including both smokers and non-smokers. Moreover, we can investigate alcoholics at 1 month of abstinence with increased statistical power, through either combining smoking and non-smoking participants or controlling subject variability by including more pertinent covariates. Using the DTI data from ALC at 1 month of abstinence, we can also try to predict relapse status at 6-9 months of abstinence with regional FA measures by comparing future relapsers to future abstainers.

The microstructural integrity of other substance using populations can be explored with the existing DTI data sets, by comparing polysubstance users to controls or alcoholics, by investigating the effects of smoking in polysubstance users, and by comparing heroin addicts to controls or the other substance using groups. These are all questions of interest to the substance use research community, as both cross-sectional and longitudinal DTI data sets in well-characterized substance users are not very common. Using the DTI data from polysubstance users at 1 month of abstinence, we should also be able to predict relapse status at 6-9 months of abstinence by comparing future relapsers and future abstainers among our polysubstance users.

Longitudinal studies can also be explored. We can investigate whether microstructural integrity in ALC improves with abstinence, comparing directly ALC at 1 week of abstinence to ALC at 1 month of abstinence and/or to ALC at 6-9 months of abstinence. This would more

directly confirm microstructural recovery in abstinent ALC, which so far has been only inferred from cross-sectional findings at two time points in recovery. Similarly, the longitudinal change of microstructural integrity in abstaining polysubstance users can be investigated, comparing polysubstance users at one month and about 4 months of abstinence.

Last but not least, we can further investigate whether cigarette smoking affects longitudinal recovery within ALC, by comparing differences between longitudinal data sets obtained from smoking and nonsmoking ALC at 1 month and at 6-9 months of abstinence. Previous research has indicated that smoking in alcoholics hinders recovery from neurobiological and cognitive deficits (for review see Durazzo et al., 2010).

Any such future investigations would prioritize analyses based on statistical power, on interest of the scientific question, and on likelihood of a significant finding. In addition, additional information can be gleaned from similar analyses by analyzing other DTI parameters that are provided within the TBSS processing framework, such as mean diffusivity (MD), axial diffusivity, and parallel diffusivity. These parameters have been shown to reflect compromise of cytoskeletal structure, myelin, or axonal density (Basser, 1995; Spielman et al., 1996).

5. Conclusion

According to earlier published TBSS analyses at 1.5T, sALC at 1 week of abstinence showed significant FA deficits compared with nonsmoking controls in ROIs of corpus callosum (body, genu, and splenium), fornix, cingulum bundle, and medial forebrain bundle. Here, we largely replicated these major findings with a separate 4T DTI data set of 1-week-abstinent sALC. In addition, uncorrected t-statistics showed significant FA deficits in sALC at 1 month of abstinence compared with smoking CON within ROIs corresponding to cingulum bundle, body of corpus callosum, fornix, and medial forebrain bundle; after FWE correction, no regional FA

difference remained. Exploratory uncorrected *t*-statistics found regions of significant FA decreases and increases in smoking ALC versus nonsmoking ALC, as well as regional FA decreases in smoking CON compared with non-smoking CON; however, after FWE correction, none of these smoking effects remained significant. To conclude, the initial analyses of these 4T DTI data sets yielded tantalizing results that require further in-depth study. They suggest that white matter microstructural integrity in alcoholics, which is compromised at 1 week of abstinence, may have partially recovered after 1 month of abstinence, and that chronic cigarette smoking may have opposite effects on regional white matter microstructural integrity in alcoholics and controls, potentially from drug interactions.

References

American Psychiatric Association (2013). *Diagnostic and Statistical Manual of Mental Disorders* (5th ed.). Arlington, VA: American Psychiatric Publishing.

Bach M, Laun FB, Leemans A, Tax CM, Biessels GJ, Stieltjes B, Maier-Hein KH (2014). Methodological considerations on tract-based spatial statistics (TBSS). *Neuroimage*; 100: 358-69.

Beaulieu C (2002). The basis of anisotropic water diffusion in the nervous system – a technical review. *NMR in Biomedicine*; 15: 435-55.

Basser PJ (1995). Inferring microstructural features and the physiological state of tissues from diffusion-weighted images. *NMR in Biomedicine*; 8(7-8): 456-467.

Bendszus M, Weijers HG, Wiesbeck G, Warmuth-Metz M, Bartsch AJ, Engels S, Böning J, Solymosi L (2001). Sequential MR imaging and proton MR spectroscopy in patients who underwent recent detoxification for chronic alcoholism: correlation with clinical and neuropsychological data. *AJNR Am J Neuroradiol*; 22(10): 1926-32.

Benedetti F, Bollettini I, Poletti S, Locatelli C, Lorenzi C, Pirovano A, Smeraldi E, Chiang GC, Zhan W, Schuff N, Weiner MW (2012). White matter alterations in cognitively normal apoE $\varepsilon 2$ carriers: insight into Alzheimer resistance? *AJNR Am J Neuroradiol*; 33(7): 1392-7.

Bolego C, Poli A, Paoletti R (2002). Smoking and gender. *Cardiovasc Res*, 53: 568-76.

Brewster RC, King TZ, Burns TG, Drossner DM, Mahle WT (2015). White Matter Integrity Dissociates Verbal Memory and Auditory Attention Span in Emerging Adults with Congenital Heart Diseases. *J Intl Neuropsychol Soc*; 21(1): 22-33.

Cardenas VA, Studholme C, Gazdzinski S, Durazzo TC, Meyerhoff DJ (2007). Deformation-based morphometry of brain changes in alcohol dependence and abstinence. *Neuroimage*; 34(3): 879-87.

Colombo C (2015). White matter microstructure in bipolar disorder is influenced by the serotonin transporter gene polymorphism 5-HTTLPR. *Gene, Brain and Behavior*; 14: 238-50.

Chanraud S, Zahr N, Sullivan EV, Pfefferbaun A (2010). MR Diffusion Tensor Imaging: A Window into White Matter Integrity of the Working Brain. *Neurophyschol Rev*; 20: 209-25.

CIND (2010). *4T EMS Process Protocol.* San Francisco VA Medical Center.

CIND (2012). *4T DTI: Teem Process Protocol.* San Francisco VA Medical Center.

CIND (2012). CIND Pre-Processing Pipeline For Diffusion Tensor Imaging. San Francisco VA Medical Center.

Cochrane J, Chen H, Conigrave KM, Hao W (2003). Alcohol Use in China. *Alcohol & Alcoholism*; 38(6): 537-42.

Durazzo TC, Gazdzinski S, Meyerhoff DJ (2007). The neurological and neurocognitive consequences of chronic cigarette smoking in alcohol use disorders. *Alcohol Alcohol*; 42(3): 174-85.

Durazzo TC, Gazdzinski S, Rothlind JC, Banys P, Meyerhoff DJ (2006). Brain metabolite concentrations and neurocognition during short-term recovery from alcohol dependence: Preliminary evidence of the effects of concurrent chronic cigarette smoking. *Alcohol Clin Exp Res*; 30(3): 539-51.

Durazzo TC, Meyerhoff DJ (2007). Neurobiological and neurocognitive effects of chronic cigarette smoking and alcoholism. *Front Biosci*; 12: 4079-100.

Durazzo TC, Meyerhoff DJ, Nixon SJ (2010). Chronic Cigarette Smoking: Implications for Neurocognition and Brain Neurobiology. *Int J Environ Res Public Health*; 7: 3760-3791.

Durazzo TC, Mon A, Gazdzinski S, Yeh PH, Meyerhoff DJ (2015). Serial longitudinal magnetic resonance imaging data indicate non-linear regional gray matter volume recovery in abstinent alcohol-dependent individuals. *Addict Biol*; 20(5): 956-67.

Durkee CA, Sarlls JE, Hommer DW, Momenan R (2013). White Matter Microstructure Alterations: A Study of Alcoholics with and without Post-Traumatic Stress Disorder. *PLoS One*; 8(11): e80952.

Garey KW, Neuhauser MM, Robbins RA, Danziger LH, Rubinstein I (2004). Markers of inflammation in exhaled breath condensate of young healthy smokers. *Chest*, 125: 22-6.

Gazdzinski S, Durazzo TC, Mon A, Yeh PH, Meyerhoff DJ (2010). Cerebral white matter recovery in abstinent alcoholics—a multimodality magnetic resonance study. *Brain*; 133(Pt 4): 1043-53.

Giovino GA (2002). Epidemiology of tobacco use in the United States. *Oncogene*; 21(48): 7326-40.

Gons RA, van Norden AG, de Laat KF, van Oudheusden LJ, van Uden IW, Zwiers MP, Norris DG, de Leeuw FE (2011). Cigarette smoking is associated with reduced microstructural integrity of cerebral white matter. *Brain*; 134(Pt 7): 2116-24.

Gu D, Wu X, Reynolds K, Duan X, Xin X, Reynolds RF, Whelton PK, He J (2004). Cigarette Smoking and Exposure to Environmental Tobacco Smoke in China: The International Collaborative Study of Cardiovascular Disease in Asia. *American Journal of Public Health*; 94(11): 1972-6.

Hawkins BT, Brown RC, Davis TP (2002). Smoking and ischemic stroke: A role for nicotine.

Trends Pharmacol. *Science*; 23: 78-82.

Hess CP, Mukherjee P (2007). Visualizing white matter pathways in the living human brain: diffusion tensor imaging and beyond. *Neuroimaging Clin N Am*; 17(4): 407-26.

Hudkins M, O'Neill J, Tobias MC, Bartzokis G, London ED (2011). Cigarette smoking and white matter microstructure. *Psychopharmacology (Berl)*; 221(2): 285-95.

Kuceyeski A, Meyerhoff DJ, Durazzo TC, Raj A (2013). Loss in connectivity among regions of the brain reward system in alcohol dependence. *Hum Brain Mapp*; 34(12): 3129-42.

Li D, Yang X, Ge Z, Hao Y, Wang Q, Liu F, Gu D, Huang J (2012). Cigarette smoking and risk of completed suicide: A meta-analysis of prospective cohort studies. *Journal of Psychiatric Research*; 46: 1257-66.

Liao Y, Tang J, Deng Q, Deng Y, Luo T, Wang X, Chen H, Liu T, Chen X, Brody AL, Hao W (2011). Bilateral fronto-parietal integrity in young chronic cigarette smokers: a diffusion tensor imaging study. *PLoS One*; 6(11): e26460.

Lin F, Wu G, Zhu L, Lei H (2013). Heavy smokers show abnormal microstructural integrity in the anterior corpus callosum: a diffusion tensor imaging study with tract-based spatial statistics. *Drug Alcohol Depend*; 129(1-2): 82-7.

Ma L, Steinberg JL, Keyser-Marcus L, Ramesh D, Narayana PA, Merchant RE, Moeller FG, Cifu DX (2015). Altered white matter in cocaine-dependent subjects with traumatic brain injury: A diffusion tensor imaging study. *Drug Alcohol Depend*; 151:128-34.

Martin PR, Gibbs Sj, Nimmerrichter AA, Riddle WR, Welch LW, Willcott MR (1995). Brain proton magnetic resonance spectroscopy studies in recently abstinent alcoholics. *Alcohol Clin Exp Res*; 19(4): 1078-82.

Meyerhoff DJ (2014). Chapter 19: Brain proton magnetic resonance spectroscopy of alcohol use disorders. *Handb Clin Neurol*; 125: 313-37.

Mon A, Durazzo TC, Gazdzinski S, Meyerhoff DJ (2009). The impact of chronic cigarette smoking on recovery from cortical gray matter perfusion deficits in alcohol dependence: longitudinal arterial spin labeling MRI. *Alcohol Clin Exp Res*; 33(8): 1314-21.

Mori S, Wakana S, Nagae-Poetscher LM, van Zijl PCM (2005). *MRI atlas of human white matter*. Elsevier; Amsterdam: Elsevier.

Mori S, Zhang J (2006). Principles of Diffusion Tensor Imaging and its Applications to Basic Neuroscience Research. *Neuron*; (51): 527-39.

Mukherjee P, Berman JI, Chung SW, Hess CP, Henry RG (2008). Diffusion Tensor MR Imaging and Fiber Tractography: Theoretic Underpinnings. *AJNR Am J Neuroradiol*; 29(4): 632-41.

Mukherjee P, Chung SW, Berman JI, Hess CP, Henry RG (2008). Diffusion Tensor Imaging and Fiber Tractography: Technical Considerations. *AJNR AM J Neuroradiol*; 29(5): 843-52.

Parks MH, Dawant BM, Riddle WR, Hartmann SL, Dietrich MS, Nickel MK, Price RR, Martin PR (2002). Longitudinal brain metabolic characterization of chronic alcoholics with proton magnetic resonance spectroscopy. *Alcohol Clin Exp Res*; 26(9): 1368-80.

Paul RH, Grieve SM, Niaura R, David SP, Laidlaw DH, Cohen R, Sweet L, Taylor G, Clark RC, Pogun S, Gordon E (2008). Chronic cigarette smoking and the microstructural integrity of white matter in healthy adults: a diffusion tensor imaging study. *Nicotine Tob Res*; 10(1): 137-47.

Pfefferbaum A, Sullivan EV (2005). Disruption of brain white matter microstructure by excessive intracellular and extracellular fluid in alcoholism: evidence from diffusion tensor imaging. *Neuropsychopharmacology*; 30: 423-32.

Pfefferbaum A, Zahr NM, Mayer D, Rohlfing T, Sullivan EV (2015). Dynamic responses of selective brain white matter fiber tracts to binge alcohol and recovery in the rat. *PLoS One*; 10(4): e0124885.

R Foundation for Statistical Computing (2012). *R: A language and environment for statistical computing.* Vienna, Austria. Retried from https://www.r-project.org/

Research Society on Alcoholism (2015). *Impact of Alcoholism and Alcohol Induced Disease and Disorders on America.*

Segobin S, Ritz L, Lannuzel C, Boudehent C, Vabret F, Eustache F, Beaunieux H, Pitel AL (2015). Integrity of white matter microstructure in alcoholics with and without Korsakoff's syndrome. *Hum Brain Mapp*; 36(7): 2795-808.

Smith SM, Jenkinson M, Johansen-Berg H, Rueckert D, Nichols TE, Mackay CE, Watkins KE, Ciccarelli O, Cader MZ, Matthews PM, Behrens TE (2006). Tract-based spatial statistics: voxelwise analysis of multi-subject diffusion data. *Neuroimage*; 31: 1487-505.

Spielman D, Butts K, de Crespigny A, Moseley M (1996). Diffusion-weighted imaging of clinical stroke. *International Journal of Neuroradiology*; 1: 44-55.

Wang Y, Li W, Li Q, Yang W, Zhu J, Wang W (2011). White matter impairment in heroin addicts undergoing methadone maintenance treatment and prolonged abstinence: a preliminary DTI study. *Neurosci Lett*; 494(1): 49-53.

Wang JJ, Durazzo TC, Gazdzinski S, Yeh PH, Mon A, Meyerhoff DJ (2009). MRSI and DTI: a multimodal approach for improved detection of white matter abnormalities in alcohol and nicotine dependence. *NMR Biomed*; 22(5): 516-22.

Yeh PH, Simpson K, Durazzo TC, Gazdzinski S, Meyerhoff DJ (2009). Tract-Based Spatial Statistics (TBSS) of diffusion tensor imaging data in alcohol dependence: abnormalities of the motivational neurocircuitry. *Psychiatry Res*; 173(1): 22-30.

Yu D, Yuan K, Zhang B, Liu J, Dong M, Jin C, Luo L, Zhai J, Zhao L, Zhao Y, Gu Y, Xue T, Liu X, Lu X, Qin W, Tian J (2015). White matter integrity in young smokers: a tract-based spatial statistics study. *Addict Biol*; Advance online publication. doi: 10.1111/adb.12237

Publishing Agreement

It is the policy of the University to encourage the distribution of all theses, dissertations, and manuscripts. Copies of all UCSF theses, dissertations, and manuscripts will be routed to the library via the Graduate Division. The library will make all theses, dissertations, and manuscripts accessible to the public and will preserve these to the best of their abilities, in perpetuity.

Please sign the following statement:

I hereby grant permission to the Graduate Division of the University of California, San Francisco to release copies of my thesis, dissertation, or manuscript to the Campus Library to provide access and preservation, in whole or in part, in perpetuity.

Author Signature   Date

2015.9.4